

Assessment of therapeutic efficacy and fate of engineered human mesenchymal stem cells for cancer therapy

Laura S. Sasportas^{a,b,1}, Randa Kasmieh^{a,b,1}, Hiroaki Wakimoto^c, Shawn Hingtgen^{a,b}, Jeroen A. J. M. van de Water^{a,b}, Gayatry Mohapatra^e, Jose Luiz Figueiredo^b, Robert L. Martuza^c, Ralph Weissleder^{b,f}, and Khalid Shah^{a,b,d,2}

^aMolecular Neurotherapy and Imaging Laboratory, ^bCenter for Molecular Imaging Research (CMIR), Department of Radiology, Departments of ^cNeurosurgery, ^dNeurology, and ^ePathology, and ^fCenter for Systems Biology, Department of Systems Biology, Massachusetts General Hospital, Harvard Medical School Boston, MA 02114

Edited by Webster K. Cavenee, University of California at San Diego School of Medicine, La Jolla, CA, and approved January 16, 2009 (received for review July 11, 2008)

The poor prognosis of patients with aggressive and invasive cancers combined with toxic effects and short half-life of currently available treatments necessitate development of more effective tumor selective therapies. Mesenchymal stem cells (MSCs) are emerging as novel cell-based delivery agents; however, a thorough investigation addressing their therapeutic potential and fate in different cancer models is lacking. In this study, we explored the engineering potential, fate, and therapeutic efficacy of human MSCs in a highly malignant and invasive model of glioblastoma. We show that engineered MSC retain their “stem-like” properties, survive longer in mice with gliomas than in the normal brain, and migrate extensively toward gliomas. We also show that MSCs are resistant to the cytokine tumor necrosis factor apoptosis ligand (TRAIL) and, when engineered to express secreted recombinant TRAIL, induce caspase-mediated apoptosis in established glioma cell lines as well as CD133-positive primary glioma cells in vitro. Using highly malignant and invasive human glioma models and employing real-time imaging with correlative neuropathology, we demonstrate that MSC-delivered recombinant TRAIL has profound anti-tumor effects in vivo. This study demonstrates the efficacy of diagnostic and therapeutic MSC in preclinical glioma models and forms the basis for developing stem cell-based therapies for different cancers.

gliomas | in vivo imaging | TRAIL

Human mesenchymal stem cells (MSCs) are multipotent cells that can self-renew, proliferate, and differentiate into a variety of cell types (1, 2). A significant improvement in understanding MSC biology in recent years has paved the way to their potential clinical use. MSCs are attractive candidates for manipulation as they can easily be isolated from patients, cultured in vitro, and autologously transplanted into patients, thus overcoming the difficulties related to immune rejection of transplanted cells (3, 4). Modified MSCs have also been shown to have high metabolic activity and strong expression of transgenes in vitro and in vivo (5).

Glioblastoma multiforme (GBM) is the most aggressive form of glioma, with a median survival time of 10 to 12 months (6). Despite considerable advances in glioma therapy, GBM remains one of the most challenging diseases, particularly because of its invasiveness, which precludes surgical removal. Glioblastomas consist of heterogeneous population of cells, some of which have been shown to extensively proliferate, self-renew, infiltrate, and be solely responsible for the growth of main tumor mass (7, 8). Direct targeting of the primary tumor mass and the disseminated deposits arising from invasive tumor cells by genetically modified stem cells could be a promising therapeutic approach.

MSCs have been shown to migrate toward gliomas (9) and track microscopic tumor deposits and infiltrating tumor cells in the brain (10, 11). Furthermore, engineered MSCs have been shown to exert potent inhibition of tumor growth in an in vivo glioma model and also exhibit a protective effect for the normal brain (12). However, most of these studies lack a thorough in vivo characterization of

engineered MSCs or their application in mouse models of cancer. We have previously engineered lentiviral vectors bearing fluorescent and bioluminescent markers to stably label stem cells and tumor cells to study their fate in real time in vitro and in vivo (13). In this study, we have explored the possibility of modifying MSCs with different combinations of fluorescent and bioluminescent markers and engineered a tumor-specific secretable form of recombinant TRAIL, S-TRAIL (14). Furthermore, we have used real-time optical imaging to follow the delivery, fate, and therapeutic efficacy of engineered MSCs and the pharmacodynamics of therapeutic MSCs in real time in both invasive and malignant mouse glioma models.

Results

Human mesenchymal stem cells (Fig. 1A) were efficiently transduced with our recently engineered lentiviral vector (LV) constructs encoding firefly luciferase (Fluc) and GFP fusion proteins (13) as revealed by GFP fluorescence (Fig. 1B) and flow cytometry (Fig. 1C). MSCs transduced with LV-GFP-Fluc retained fusion protein expression through 3 weeks (Fig. 1D) and had a slightly reduced proliferation rate compared with non-transduced cells over several passages in culture (transduced cells at day 2; $88\% \pm 5\%$; day 9, $83\% \pm 4\%$; day 16, $82\% \pm 4\%$) [supporting information (SI) Fig. S1A]. Genomic profiles generated by array comparative genomic hybridization confirmed normal DNA copy number in transduced (Fig. 1E) and non-transduced MSCs (data not shown). Karyotype analysis performed on transduced (Fig. 1F) and non-transduced MSC (data not shown) ruled out chromosomal rearrangements in lentiviral-transduced cells. These experiments demonstrate that MSCs can be efficiently and stably transduced with LV and that LV modification does not result in altering DNA copy number and arrangement of MSCs.

To determine MSC survival in vivo, we used MSCs expressing GFP-Fluc. A direct correlation between cell number of the GFP-Fluc-expressing MSCs and Fluc signal intensity in vitro (Fig. S1C) and in vivo (Fig. S1D) within the ranges tested was observed. Next, MSC-GFP-Fluc or a mix of MSC-GFP-Fluc and human glioma cells Gli36-EGFRvIII were implanted in the brain parenchyma and survival was followed in real time by bioluminescence imaging. As shown in the summary graph and representative images (Fig. 1G), MSC survival was increased in the presence of glioma cells compared with the MSCs implanted without glioma cells (day 14, MSCs

Author contributions: K.S. designed research; L.S.S., R.K., H.W., S.H., J.A.J.M.v.d.W., G.M., J.L.F., and K.S. performed research; R.L.M. contributed new reagents/analytic tools; L.S.S., R.K., H.W., S.H., G.M., R.W., and K.S. analyzed data; and L.S. and K.S. wrote the paper.

The authors declare no conflict of interest.

This article is a PNAS Direct Submission.

¹L.S.S. and R.K. contributed equally to this work.

²To whom correspondence should be addressed. E-mail: kshah@helix.mgh.harvard.edu.

This article contains supporting information online at www.pnas.org/cgi/content/full/0806647106DCSupplemental.

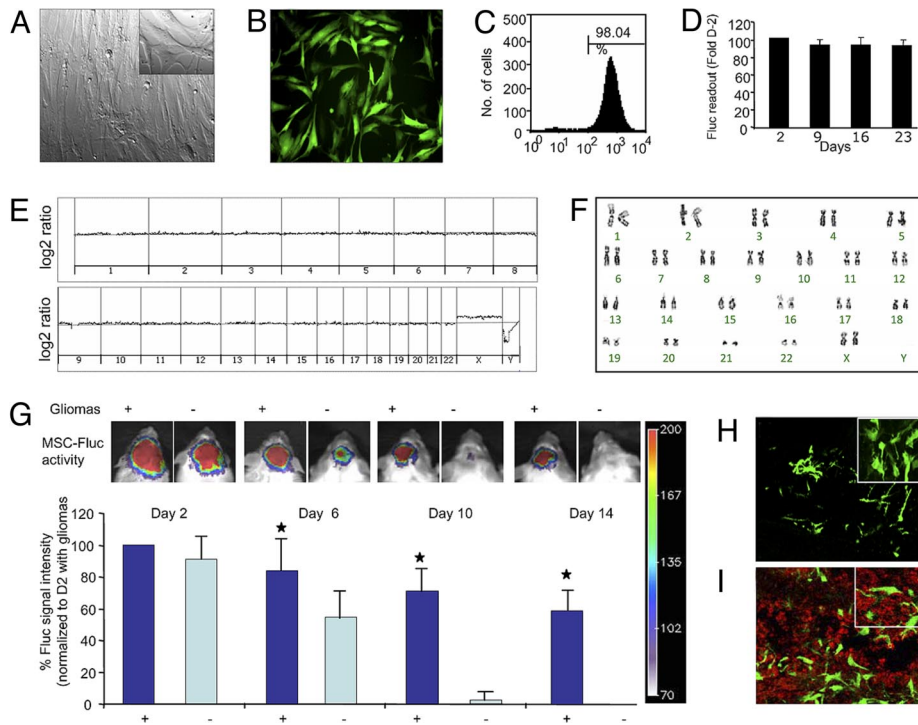


Fig. 1. Transduced human MSCs proliferate in culture and survive longer in mice bearing gliomas. (A) Light image of MSCs in culture. (B–D) MSCs were transduced with LV-GFP-Fluc and, 48 h later, were FACS-sorted. Photomicrograph of MSCs expressing GFP-Fluc (B). (C) Plot showing the percentage of transduced MSCs expressing GFP. (D) In vitro imaging shows the expression of Fluc in MSC-GFP-Fluc over time. (E) Genomic profiles of transduced MSCs. (F) Karyotype analysis of transduced MSCs. (G) Fluc bioluminescence intensities of MSC-GFP-Fluc implanted intraparenchymally either alone or mixed with Gli36-EGFRvIII human glioma cells. One representative image of mice with MSC-GFP-Fluc implanted with (+) or without (-) glioma cells is shown. (H and I) Photomicrographs on brain sections from mice 16 days after implantation shows presence of GFP-positive MSCs in normal brain (H) and the presence of Ki67-positive glioma cells (red) and GFP-positive MSCs in glioma bearing brains (I). (Original magnification: B, H, and I, $\times 20$.)

without gliomas, 0%; with gliomas, $60\% \pm 12\%$). Furthermore, the presence of GFP-expressing MSCs in day-6 brain sections from mice implanted with MSCs only (Fig. 1H) and GFP-expressing MSCs and Ki67-positive glioma cells in day-14 brain sections from mice implanted with MSCs with gliomas (Fig. 1I) confirmed the presence of MSCs in the brain. These results indicate that glioma cells or host response modulates MSC survival in the brain after transplantation.

Evidence suggests that MSCs may influence tumor progression in several tumor types (15–17). To determine the effect of engineered MSCs on glioma growth, we created a human glioma line Gli36-EGFRvIII expressing Fluc-DsRed2 (Gli36-EGFRvIII-FD) by transducing glioma cells with LV-Fluc-Dsred2. A direct correlation between glioma cell number and Fluc signal intensity was seen in vitro within the ranges tested (Fig. S1B). We implanted Gli36-EGFRvIII-FD, or a mix of Gli36-EGFRvIII-FD and MSC-GFP and followed glioma growth in real time. As shown in the summary graph and representative images (Fig. 2A), there was no significant effect of MSCs on glioma growth over time. Furthermore, the presence of DsRed2 and both DsRed2 and GFP in day-16 brain sections from mice implanted with glioma cells only (Fig. 2B) and with glioma cells and MSC-GFP (Fig. 2C), respectively, confirmed the presence of tumor cells and MSCs in mouse brains.

These results indicate that MSCs have no significant influence on the progression of gliomas in the brain.

The formation of gap junctions between potential therapeutic cells and tumor cells has been shown to be critical for bystander effect, and this gap junction-mediated communication between cells can be measured by flow cytometry using a membrane bound marker, DI1, and a non-permeable marker, calcein-AM (18). Human Gli36-EGFRvIII glioma cells were labeled with DI1 and MSCs were labeled with calcein-AM. Two distinct populations of red (DI1-labeled) and green (calcein-AM) cells were seen immediately after mixing labeled MSCs and glioma cells (Fig. 3A, C, and D). However, after 3 h of incubation, a double-positive red and green fluorescent population of DI1-labeled glioma cells was seen (Fig. 3B, E, and F), whereas no green fluorescence was found in MSCs as a result of the transfer of calcein-AM. To study homing of MSCs in a mouse model of glioma, MSCs were transduced with LV-tdTomato and Gli36-EGFRvIII human glioma cells were transduced with LV-GFP-Fluc. MSCs expressing tdTomato (Fig. 3G) were implanted at a 1-mm distance from established human gliomas expressing GFP-Fluc (Fig. 3H). Fluorescence confocal microscopy on brain sections from mice 2 and 10 days after implantation confirmed the homing of tdTomato MSCs toward the GFP-positive gliomas and not in the surrounding normal brain

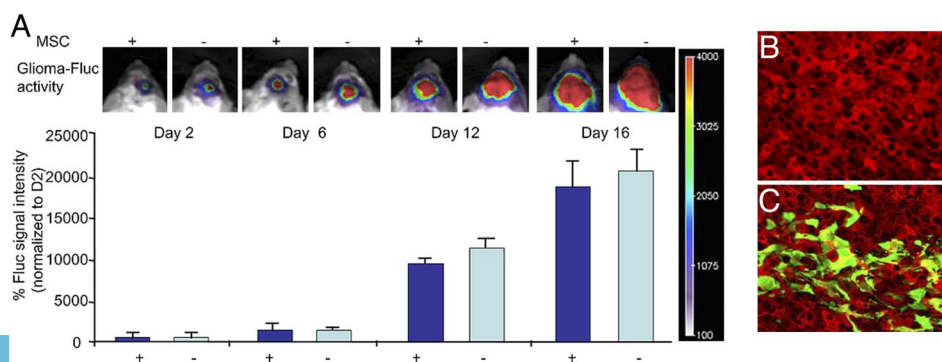


Fig. 2. Human MSCs do not influence glioma growth in mice. (A) Fluc bioluminescence intensities of intraparenchymally implanted mice with Gli36-EGFRvIII-FD human glioma cells or a mix of Gli36-EGFRvIII-FD and MSC-GFP. One representative image of mice with Gli36-EGFRvIII-FD implanted with (+) or without (-) MSC-GFP is shown. (B and C) Photomicrographs on brain sections from mice 16 days after implantation shows expression of DsRed2 in glioma cells (B) and the presence of GFP-positive MSCs in mice bearing gliomas (C). (Original magnification: B and C, $\times 20$.)

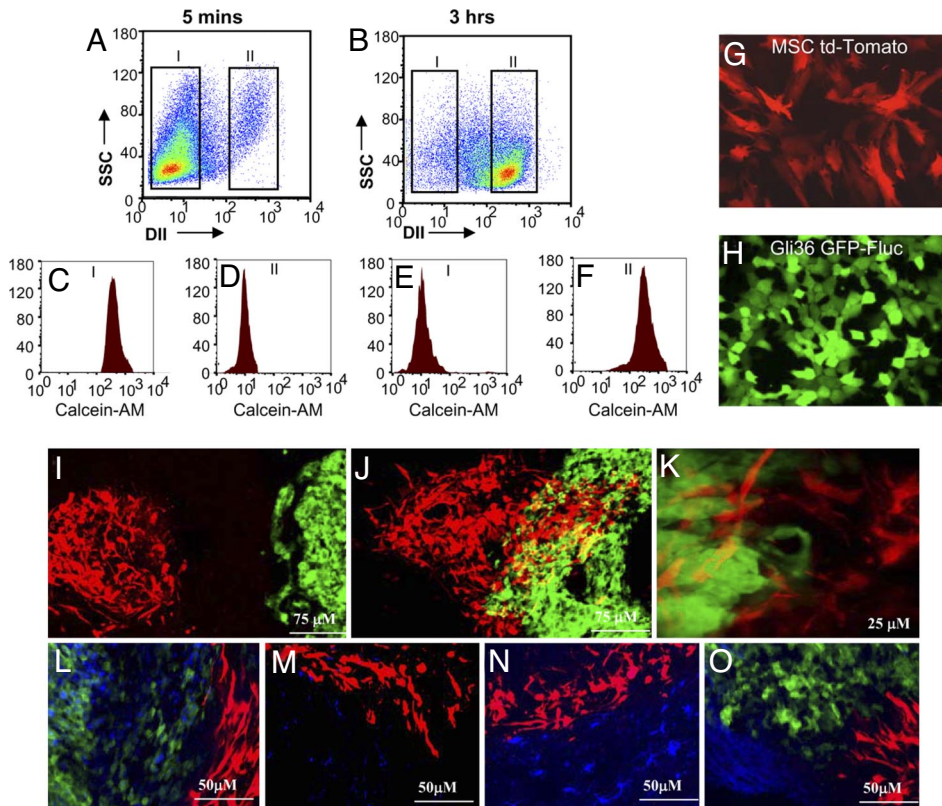


Fig. 3. Bystander effect and migration of MSCs. (A–F) Human Gli36-EGFRvIII glioma cells were labeled with DII and MSCs were labeled with calcein-AM, mixed, and FACS-sorted after 5 min and after 3 h. FACS-sorted plots and graphs reveal different populations of labeled cells after 5 min (A, C, and D) and 3 h (B, E, and F). (G and H) Photomicrographs of MSCs expressing tdTomato (G) and human Gli36-EGFRvIII glioma cells expressing GFP-Fluc (H). MSCs expressing tdTomato were implanted intracranially at a 1-mm distance from established human gliomas expressing GFP-Fluc. (I and J) Photomicrographs showing MSC-tdTomato (red) and gliomas (green) on day 2 (I) and day 10 (J) in brain sections and by intravital microscopy on day 10 after MSC implantation (K). (L–O) Immunohistochemistry on day-14 brain sections from Gli36-EGFRvIII-glioma bearing mice implanted with MSCs expressing tdTomato. Representative images of brain sections immunostained for Ki67 (L), nestin (M), GFAP (N), and MAP-2 (O). (Green, GFP expression; blue, nestin, Ki67, GFAP, or MAP-2 expression; original magnification: I and J, $\times 10$; K–O, $\times 20$.)

tissue (Fig. 3 I and J). Intravital microscopy confirmed the robust migration of MSCs toward and into gliomas within 10 days of MSC implantation (Fig. 3K). Immunohistochemical analysis on brain sections from mice bearing gliomas and implanted with MSCs expressing tdTomato 2 weeks after implantation showed no expression of the proliferation marker Ki67 (Fig. 3L), the neural stem cell marker nestin (Fig. 3M), the astrocytic marker GFAP (Fig. 3N), or the neuronal marker MAP-2 (Fig. 3O) in MSCs. In contrast, robust Ki67 expression was seen in glioma cells (Fig. 3L), and GFAP (Fig. 3N) and MAP-2 (Fig. 3O) expression was seen in normal brain. These results show that MSCs implanted in the mice with established glioma home to tumors, do not proliferate, and remain in un-differentiated state.

To verify whether MSCs can serve as cellular vehicles to deliver a secretable form of TRAIL, we first evaluated the expression of death domain-containing TRAIL binding receptor, TRAIL-R1 (DR4), on both MSCs and glioma cells. Immunoreactive proteins of expected size were present in the glioma cells and absent in the MSCs (Fig. 2A). Dose-response curves confirmed that there was no effect of S-TRAIL on MSC viability, whereas Gli36-EGFRvIII cell viability was reduced to 60% at 100 ng/mL and to 20% at 300 ng/mL S-TRAIL 24 h after incubation (Fig. 2B). To convert MSCs into therapeutic vehicles, we transduced MSCs with LV-S-TRAIL. A high number of transduced cells was revealed by GFP fluorescence (Fig. 2C) and FACS sorting (Fig. S2D). Quantification of TRAIL in the cell culture medium confirmed secretion of 250 ng/10⁶ cells/24 h by MSCs with no significant amounts produced by control cells (Fig. S2E). Furthermore, Gli36-EGFRvIII cells exposed to conditioned medium from MSC-S-TRAIL and MSC-GFP showed activation of caspases (Fig. S2 F–J) and PARP (Fig. S2H) and resulted in glioma cell killing in a dose-dependent manner (Fig. S2I) in MSC-S-TRAIL and not MSC-GFP-treated cells (Fig. S2J). These results show that MSCs are resistant to TRAIL and engineered MSCs secrete S-TRAIL that induces caspase-mediated apoptosis in glioma cells in culture.

To follow stability and duration of S-TRAIL secretion in vivo, we used a recently engineered N-terminal *Gaussia* luciferase (Gluc) fusion of S-TRAIL (19). Gluc is a naturally secreted bioluminescent protein that is well suited for extra-cellular detection as it does not require ATP for its activity (20). Gluc bioluminescence imaging on MSCs transduced with LV-Gluc-S-TRAIL showed that MSCs secreted Gluc-S-TRAIL in the culture medium (Fig. 4A). To simultaneously track MSCs survival and S-TRAIL secretion in vivo, MSCs were co-transduced with LV-Gluc-S-TRAIL and LV-GFP-Fluc. A linear correlation between the Gluc activity depicting S-TRAIL secreted in the culture medium and the Fluc activity depicting the number of MSCs secreting S-TRAIL was shown by dual in vitro bioluminescence imaging (Fig. 4A). When a mix of human glioma cells, Gli36-EGFRvIII, and GFP-Fluc MSCs secreting Gluc-S-TRAIL was implanted s.c. in mice, dual bioluminescence imaging revealed that both MSCs and the release of S-TRAIL from MSCs can be detected in vivo (Fig. 4B). Furthermore, S-TRAIL expression is continuous and stable over time for at least 2 weeks (Fig. 4B). These experiments demonstrate that kinetics of both the apoptotic agent and the delivery vehicle can be followed in real time in vivo. Furthermore, these experiments also demonstrate that tumor cells have the prolonged access to the S-TRAIL delivered by MSCs in vivo.

To assess the effect of S-TRAIL delivered via engineered MSCs on the formation of gliomas, we used the human glioma line Gli36-EGFRvIII-FD. Serial Fluc bioluminescence imaging on mice implanted with a mix of Gli36-EGFRvIII-FD and S-TRAIL or control GFP expressing MSCs (3:1 ratio) revealed a significant reduction in glioma burden in animals bearing MSCs expressing S-TRAIL compared with controls ($P < 0.001$; Fig. 4 C–I). Histopathological analysis on day-6 brain sections revealed the presence of a significantly higher number of activated caspase-3-positive cells in MSC-S-TRAIL-treated tumors and not in MSC-GFP-treated tumors (Fig. 4 J–L). Also, a significant decrease in the number of proliferating tumor cells was seen in MSC-S-TRAIL-treated tumors compared to the controls (Fig. 4 M–O). These

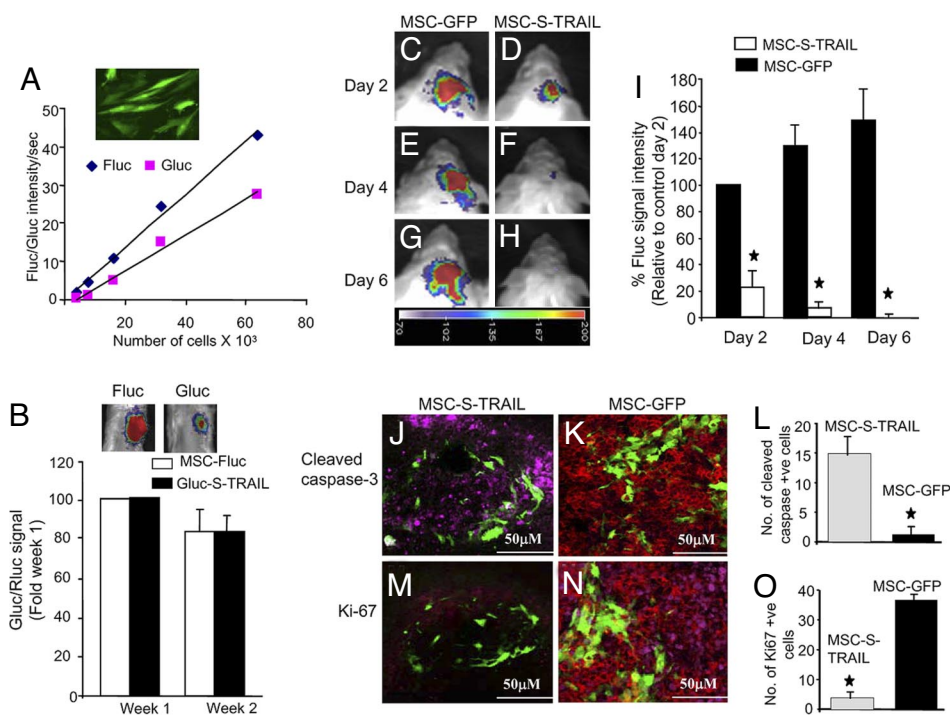


Fig. 4. Pharmacodynamics and therapeutic efficacy of MSC-S-TRAIL. (A) MSCs were co-transduced with LV-Gluc-S-TRAIL and LV-GFP-Fluc, and cells and conditioned culture medium were imaged for Fluc and Gluc activity, respectively. Plots show correlation between the different concentrations of cells-Fluc activity and medium-Gluc activity within the ranges tested. (B) MSCs expressing Gluc-S-TRAIL and GFP-Fluc were mixed with Gli36-EGFRvIII glioma cells and implanted s.c. in nude mice. Mice were imaged for Fluc and Gluc activity every week for a period of 2 weeks. (C–H) Serial in vivo bioluminescence imaging of tumor growth following intracranial implantation of Gli36-EGFRvIII-FD glioma cells mixed with MSCs expressing S-TRAIL (MSC-S-TRAIL; D, F, and H) or GFP (MSC-GFP; C, E, and G). One representative mouse image from each group is shown. (I) Relative mean bioluminescent signal intensities after quantification of in vivo images. (J–O) Photomicrographs show presence of cleaved caspase-3 (J) and Ki67-positive cells (M) in brain sections from MSC-S-TRAIL-treated and control mice (K and N) 6 days after implantation. Plot shows the number of cleaved caspase-3 (L) and Ki67 (O) cells in MSC-S-TRAIL and MSC-GFP-treated tumors. (Green, MSCs; red, glioma cells; purple, Ki67 or cleaved caspase-3 expression; original magnification: J, K, M, and N, $\times 20$.)

results show that MSC-delivered S-TRAIL strongly inhibits tumor growth in vivo by activation of caspase-mediated apoptosis.

To assess the effect of S-TRAIL on established gliomas, we characterized a CD133-positive human primary brain tumor cell line (GBM8) for its DR4, Akt, and PTEN status (Fig. 5A). GBM8 cells expressed a higher level of DR4 and pAkt than Gli36 human glioma cells. GBM8 cells exposed to conditioned medium from MSC-S-TRAIL showed activation of caspase-3 (Fig. 5B and C) and resulted in glioma cell killing in a dose-dependent manner (Fig. 5D). To follow GBM8 cells in vivo, we transduced GBM8 cells with LV-GFP-Fluc. Flow cytometry analysis on GBM8-GFP-Fluc cells stained with phycoerythrin-conjugated anti-CD133/2 antibody revealed a high percentage of cells expressing stem cell marker CD133 in transduced GBM8 (Fig. S3A). A direct correlation between GBM8-GFP-Fluc cell number and Fluc signal intensity was seen in vitro within the ranges tested (Fig. S3B). Transduced GBM8 stained positive for nestin (Fig. 5E) and GFAP (Fig. 5F), thus retaining the characteristics of GBM8. Histopathological analysis on the sections from the brain with GBM8 implantation also confirmed their capability of forming invasive tumors in vivo (Fig. 5G and H). Next, mice bearing established GBM8-GFP-Fluc gliomas were implanted with MSC-S-TRAIL or control MSC-DsRed2 and serial Fluc bioluminescence imaging was performed every 2 weeks for a period of 5 weeks. As a result of the diffuse and invasive nature of GBM8 cells, no Fluc signal could be seen until week 3 of glioma cell implantation in both control and MSC-S-TRAIL-treated tumors (data not shown). A significant Fluc signal intensity revealing the growth of GBM8 in the brain was seen in MSC-DsRed2 control-treated mice at 3 and 5 weeks, whereas mice implanted with MSC-S-TRAIL showed no Fluc signal ($P < 0.001$; Fig. 5J). Kaplan-Meier survival analysis revealed statistically significant prolongation of survival in the group receiving MSC-S-TRAIL (median survival time, 72 d) compared with the group with control MSC (median survival time, 54.5 d; log-rank test, $P < 0.005$; Fig. 5J). Histopathological analysis on brain sections revealed the presence of MSCs (Fig. 5K) and a significantly higher number of proliferating glioma cells in MSC-DsRed2-treated mice than in MSC-S-TRAIL-treated mice (Fig. 5L–N). Furthermore, a significantly higher number of activated caspase-3-positive cells was seen

in MSC-S-TRAIL-treated gliomas compared with MSC-DsRed2-treated gliomas (Fig. 5O and P). These results show that MSC-delivered S-TRAIL induces apoptosis in highly invasive tumor cells, thus leading to a significant increase in survival times in mice.

Discussion

In this study, we have explored the possibility of engineering human MSCs with diagnostic and therapeutic proteins to study their fate and therapeutic efficacy in 2 different mouse models of glioma. We show that engineered human MSCs retain their characteristics, home to glioma tumors, and have significant anti-tumor effect on both malignant and invasive primary gliomas in vivo.

Stem and progenitor cell-mediated gene delivery is emerging as a strategy to improve the efficacy and minimize the toxicity of current gene therapy approaches. Multiple potential sources for clinically useful stem and progenitor cells have been identified, including autologous and allogeneic embryonic cells and fetal and adult somatic cells from neural, adipose, and mesenchymal tissues. MSCs harvested from bone marrow are easy to obtain and highly proliferative, allowing autologous transplantation without any need for immuno-suppression, and, in contrast to embryo-derived stem cells, MSCs pose few ethical problems. Because of their high amphotrophic receptor levels, MSCs are readily transducible with integrating vectors and lead to stable transgene expression in vitro and in vivo (20). Recent studies have shown that lentiviral transduction is more efficient than onco-retroviral transduction and improves engraftment of MSCs (21) without affecting their stem cell properties (22). In this study, we have shown that human MSCs can be efficiently transduced with bi-modal lentiviral vectors and engineered MSCs maintain transgene expression and can be cultured long-term in vitro, without losing their “stem-ness.” Furthermore, our studies reveal that engineered MSCs retain transgene expression in vivo; however, their survival is affected by the presence of glioma tumors in the brain. This can be attributed to the secretion of a number of bioactive growth factors and cytokines, such as VEGF, transforming growth factor- β , or IL-10 (23, 24), secreted by the tumor microenvironment, which have been shown to exert a profound immunosuppressive activity on antigen-presenting cells and T-effector cells. Tumors are also known to be

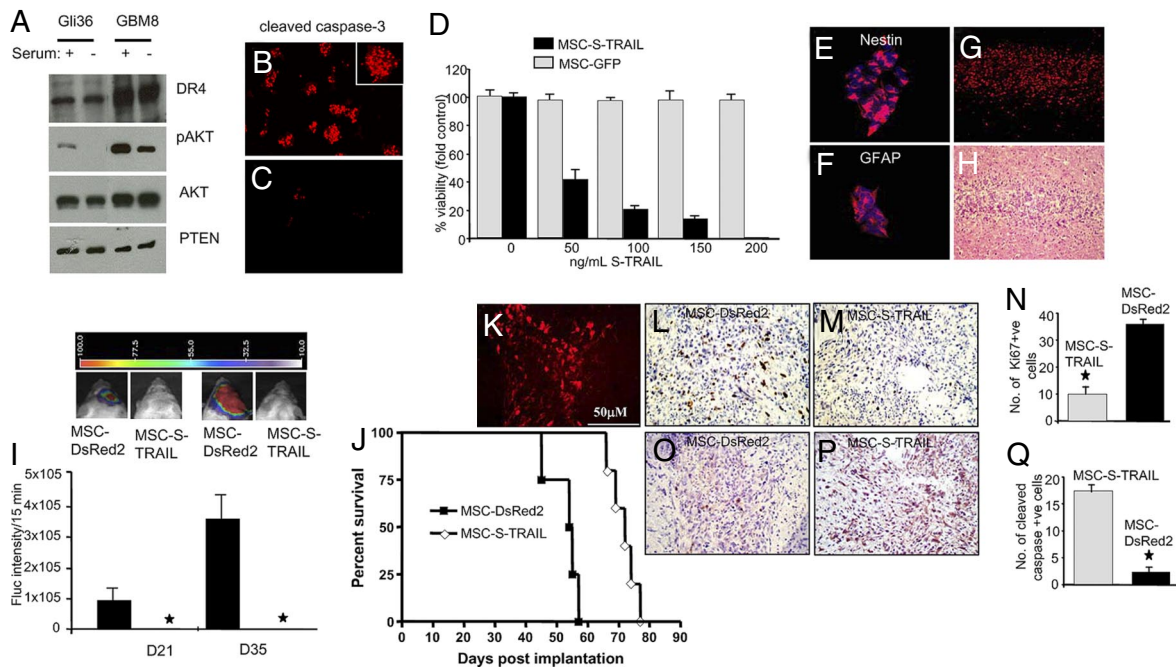


Fig. 5. Molecular profiling of primary brain tumor cells and therapeutic efficacy of MSC-S-TRAIL in primary brain tumor cells. (A) Western blot analysis of the lysates of CD133-positive human primary glioma cell line (GBM8) and human Gli36 glioma line (B and C) GBM8 cells were incubated with the conditioned medium from MSC-S-TRAIL and, 18 h later, cells were stained with anti-cleaved caspase-3 antibody. Photomicrograph shows S-TRAIL-treated (B) and control-treated cells (C). (D) Cell viability of GBM cells incubated with different concentrations of S-TRAIL. (E and F) Photomicrographs of GFP-Fluc-expressing GBM8 cells stained with anti-nestin (E) and anti-GFAP antibodies (F). (G and H) Photomicrographs of day-14 brain sections stained with anti-human nuclei (G) and H & E (H) from mice bearing GBM8-GFP-Fluc gliomas. (I) Plots of photon intensities from MSC-S-TRAIL or MSC-DsRed2 established GBM8-GFP-Fluc glioma-treated tumors at weeks 3 and 5 of implantation are shown. (J) Survival curves of GBM8-GFP-Fluc-bearing mice treated with MSC-DsRed2 and MSC-S-TRAIL. (K–M) Photomicrographs showing presence of DsRed2 MSCs in brain sections from control mice (K) and Ki67 (L and M) and cleaved caspase-3 (O and P) cells in brain sections from control and MSC-S-TRAIL mice 2 weeks after the second MSC implantation. (N and Q) Plot shows the number of Ki67 (N) and cleaved caspase-3 (Q) cells in MSC-S-TRAIL- and MSC-DsRed2-treated tumors. (Original magnification: B, G, and H, $\times 10$; E, F, K–M, O, and P, $\times 20$.)

infiltrated by regulatory T cells and myeloid suppressor cells, which actively inhibit T cell responses at the tumor site through direct cell-cell contact (25), secretion of nitric oxide, or reactive oxygen species (24). All these factors favor conditions that allow tumors—and might also allow tumor-associated MSCs in our model—to escape immune recognition and foster their proliferation and survival. A number of studies have shown enhancement of tumor growth and development, potentially through immunomodulatory and pro-angiogenic properties of MSCs, whereas others have shown no apparent effect of MSCs or have demonstrated inhibition of tumor growth and extended survival (15–17). Our results indicate that MSCs have no significant influence on the progression of gliomas in the brain.

In this work, we demonstrate that MSCs are able to migrate to tumors in a mouse model of human glioblastoma, remain in an un-differentiated state, and do not proliferate. This is in line with our previous studies on human neural stem cells (13) and the recent studies by Miletic et al. on exogenously administered MSCs in a mouse glioma model (10). Although MSCs have been shown to migrate to glioma tumors in mouse models, the molecular mechanisms underlying the glioma-directed migration of MSCs have not yet been completely elucidated. Based on previous studies on stem cell homing to lesions and tumors, a number of cytokine/receptor pairs including SDF-1/CXCR4, SCF/c-Kit, HGF/c-Met, VEGF/VEGF receptor MCP-1/CCR2, and HMGB1/RAGE (26–32) and adhesion molecules, $\beta 1$ - and $\beta 2$ -integrins, and L-selectin (28) have been associated with the tropism of stem/progenitor cells. MSCs are known to functionally express various chemokine receptors such as CCR1, CCR4, CCR7, CCR9, CCR10, CXCR4, CXCR5, CXCR6, CX3CR1, and c-met, which might be responsible for the homing of MSCs in different organs following tissue damage (28, 33). Recent

studies by Birnbaum et al. (34) show that IL-8, TGF- $\beta 1$, and NT-3 (besides VEGFA) mediate MSC recruitment by glioma.

A number of studies have shown the therapeutic effect of MSCs in mouse models of cancer. MSCs have been used for delivery of therapeutic cytokines like IFN- β (9), IL-12 (11, 35), cytosine deaminase (36), and oncolytic adenovirus (37). The ability of TRAIL to selectively target tumor cells while remaining harmless to most normal cells (38–40) makes it an attractive candidate for an apoptotic therapy in highly malignant brain tumor treatment. TRAIL signals via two pro-apoptotic death receptors (DR4 and DR5), inducing a caspase-8-dependent apoptotic cascade in tumor cells (38) However, because of its short biological half-life and limited delivery across the blood-brain barrier, most promising studies using TRAIL lack applicability (41, 42). In an established glioma model, most of the tumor cells lose the ability to proliferate and self-renew by differentiating during the first stages and creating the phenotypical signature of the tumor (43). It has been shown that CD133-positive primary brain tumor cells are essential in maintaining the growth of brain tumors (8). Our results reveal that MSCs secreting S-TRAIL induce caspase-3-mediated apoptosis in GBM8 cells, a CD133-positive primary brain tumor cell line in vitro, and, when implanted into established GBM8 tumors, resulted in a significant increase in survival of mice bearing gliomas. These results reveal that MSC-S-TRAIL cytotoxic therapy is highly efficient in inducing apoptosis in the “proliferating and maintaining” fraction in established non-xenographic gliomas. As opposed to systemic delivery of therapeutic agents, MSCs have the advantages of offering a continuous and concentrated local delivery of secretable therapeutic molecules like TRAIL, thus reducing the non-selective targeting, and allowing higher treatment efficiency and potency for a longer time period.

A number of previous studies by others and ourselves (4, 13, 14, 44, 45) have shown that in vivo bioluminescence imaging of tumor cells enables rapid, noninvasive measurement of tumor load before, during, and after treatment of mice with highly malignant intracranial tumors. Despite the advantages and convenience of bioluminescence imaging for monitoring tumor growth, there are some disadvantages that should be taken into account while assessing the fate of tumors in vivo. The light transmission is attenuated by tissue; therefore, the number of luciferase-expressing cells and their localization within the body is critical to obtain a detectable signal to follow the fate of cells in vivo—the deeper the tumors within the body (or if they are intracranial tumors), the greater the signal attenuation. In our studies on invasive glioma cells, we show that luciferase signal is undetectable in control tumors to 2 weeks and is not detectable at all in MSC-S-TRAIL-treated tumors. This could be a result of the dispersed nature of the GBM cells that are shielded by the cranium and are undetectable by luciferase imaging.

In conclusion, our studies reveal the fate and therapeutic efficacy of engineered MSCs in a mouse model of glioma using engineered lentiviral vectors and novel imaging methods. Using this study as a template, advances can be made in the way stem cells can be engineered and used in clinics in patients with brain tumors. We envision neurosurgical removal of the main tumor mass at the time of surgery and implantation of the patient's own therapeutically engineered MSCs in the resection cavity of the tumor. These MSCs would result in killing of both residual and invasive tumor cells.

Materials and Methods

Generation of Lentiviral Vectors. The following lentiviral vectors were used in this study: LV-GFP-Fluc, LV-Fluc-DsRed2 (13) and LV-tdTomato (van Ekelén, personal

communication), LV-S-TRAIL (4), and LV-Gluc-STRAIL (van Ekelén, personal communication). Both LV-S-TRAIL and LV-Gluc-S-TRAIL has an IRES-GFP element in the backbone. All lentiviral constructs were packaged as lentiviral (LV) vectors in 293T/17 cells using a helper virus-free packaging system as described (46). The transduction of MSC and glioma cells is described in detail in *SI Text*.

Cell Lines and Cell Culture. Human bone marrow-derived mesenchymal stem cells (MSC) (kindly provided by David Prockop, Tulane University, New Orleans) were grown in Alpha-MEM (Invitrogen/GIBCO) with 16.5% FBS 2–4 mM L-glutamine and penicillin/streptomycin. Human glioma cells, Gli36 expressing a constitutively active variant of EGFR (Gli36-EGFRvIII), and Gli36EGFRvIII engineered to express Fluc-DsRed2 (Gli36-EGFRvIII-FD) and 293T/17 cells were grown as described (45). GBM8 glioma cells were derived from surgical specimens of glioblastoma collected at Massachusetts General Hospital (GBM series) with approval by the Institutional Review Board. Mechanically minced tissues were digested as described in ref. 47 and were grown as “neurospheres” in Neurobasal medium (Invitrogen/GIBCO) supplemented with 3 mM L-glutamine (Mediatech), $1 \times B27$ (Invitrogen/GIBCO), 2 $\mu\text{g}/\text{mL}$ heparin (Sigma), 20 ng/ml human EGF (R and D Systems), and 20 ng/ml human FGF-2 (Peprotech).

Statistical Analysis. Data were analyzed by Student's *t* test when comparing 2 groups and by ANOVA, followed by Dunnett's post-test when comparing greater than 2 groups. Data were expressed as mean \pm SEM, and differences were considered significant at $P < 0.05$. Survival times of the mouse groups treated with MSC-S-TRAIL and MSC-DsRed2 were compared using the log-rank test.

Other methods are described in detail in *SI Text*.

ACKNOWLEDGMENTS. We thank Rainer Koehler for his help with intravital microscopy and Fil Swirski for his help with FACS analysis. This work was supported by grants from the American Brain Tumor Association (K.S.), Goldhirsh Foundation (K.S.), Alliance for Cancer Gene Therapy (K.S.), and American Cancer Society (K.S.), and by National Institutes of Health Grant P50 CA86355 (to R.W.).

- Jiang Y, et al. (2002) Pluripotency of mesenchymal stem cells derived from adult marrow. *Nature* 418:41–49.
- Mareschi K, et al. (2006) Expansion of mesenchymal stem cells isolated from pediatric and adult donor bone marrow. *J Cell Biochem* 97:744–754.
- Aboudy KS, Najbauer J, Danks MK (2008) Stem and progenitor cell-mediated tumor selective gene therapy. *Gene Ther* 15:739–752.
- Corsten MF, et al. (2007) MicroRNA-21 knockdown disrupts glioma growth in vivo and displays synergistic cytotoxicity with neural precursor cell delivered S-TRAIL in human gliomas. *Cancer Res* 67:8994–9000.
- Pereboeva L, Komarova S, Mikheeva G, Krasnykh V, Curjel DT (2003) Approaches to utilize mesenchymal progenitor cells as cellular vehicles. *Stem Cells* 21:389–404.
- Sathornsumetee S, Rich JN (2006) New approaches to primary brain tumor treatment. *Anticancer Drugs* 17:1003–1016.
- Calabrese C, et al. (2007) A perivascular niche for brain tumor stem cells. *Cancer Cell* 11:69–82.
- Singh SK, et al. (2004) Identification of human brain tumour initiating cells. *Nature* 432:396–401.
- Nakamizo A, et al. (2005) Human bone marrow-derived mesenchymal stem cells in the treatment of gliomas. *Cancer Res* 65:3307–3318.
- Miletic H, et al. (2007) Bystander killing of malignant glioma by bone marrow-derived tumor-infiltrating progenitor cells expressing a suicide gene. *Mol Ther* 15:1373–1381.
- Nakamura K, et al. (2004) Antitumor effect of genetically engineered mesenchymal stem cells in a rat glioma model. *Gene Ther* 11:1155–1164.
- Hamada H, et al. (2005) Mesenchymal stem cells (MSC) as therapeutic cytoreagents for gene therapy. *Cancer Sci* 96:149–156.
- Shah K, et al. (2008) Bimodal viral vectors and in vivo imaging reveal the fate of human neural stem cells in experimental glioma model. *J Neurosci* 28:4406–4413.
- Shah K, Tung CH, Yang K, Weissleder R, Breakefield XO (2004) Inducible release of TRAIL fusion proteins from a proapoptotic form for tumor therapy. *Cancer Res* 64:3236–3242.
- Karnoub AE, et al. (2007) Mesenchymal stem cells within tumour stroma promote breast cancer metastasis. *Nature* 449:557–563.
- Lu Y, et al. (2008) The growth inhibitory effect of mesenchymal stem cells on tumor cells in vitro and in vivo. *Cancer Biol Ther* 7:245–251.
- Yu JM, Jun ES, Bae YC, Jung JS (2008) Mesenchymal stem cells derived from human adipose tissues favor tumor cell growth in vivo. *Stem Cells Dev* 17:463–473.
- Czyz J, Irmur U, Schulz G, Mindermann A, Hulser DF (2000) Gap-junctional coupling measured by flow cytometry. *Exp Cell Res* 255:40–46.
- Verhaegent M, Christopoulos TK (2002) Recombinant Gaussia luciferase. Overexpression, purification, and analytical application of a bioluminescent reporter for DNA hybridization. *Anal Chem* 74:4378–4385.
- Lee K, et al. (2001) Human mesenchymal stem cells maintain transgene expression during expansion and differentiation. *Mol Ther* 3:857–866.
- Van Damme A, et al. (2006) Efficient lentiviral transduction and improved engraftment of human bone marrow mesenchymal cells. *Stem Cells* 24:896–907.
- Chan J, et al. (2005) Human fetal mesenchymal stem cells as vehicles for gene delivery. *Stem Cells* 23:93–102.
- Maeurer MJ, et al. (1995) Host immune response in renal cell cancer: interleukin-4 (IL-4) and IL-10 mRNA are frequently detected in freshly collected tumor-infiltrating lymphocytes. *Cancer Immunol Immunother* 41:111–121.
- Vieweg J, Su Z, Dahm P, Kusmartsev S (2007) Reversal of tumor-mediated immunosuppression. *Clin Cancer Res* 13(suppl):7275–7325.
- Zou W (2006) Regulatory T cells, tumour immunity and immunotherapy. *Nat Rev Immunol* 6:295–307.
- Ehteshami M, et al. (2002) Induction of glioblastoma apoptosis using neural stem cell-mediated delivery of tumor necrosis factor-related apoptosis-inducing ligand. *Cancer Res* 62:7170–7174.
- Imitola J, et al. (2004) Directed migration of neural stem cells to sites of CNS injury by the stromal cell-derived factor 1alpha/CXC chemokine receptor 4 pathway. *Proc Natl Acad Sci USA* 101:18117–18122.
- Son BR, et al. (2006) Migration of bone marrow and cord blood mesenchymal stem cells in vitro is regulated by stromal-derived factor-1-CXCR4 and hepatocyte growth factor-c-met axes and involves matrix metalloproteinases. *Stem Cells* 24:1254–1264.
- Heese O, Disko A, Zirkel D, Westphal M, Lamszus K (2005) Neural stem cell migration toward gliomas in vitro. *Neuro Oncol* 7:476–484.
- Schmidt NO, et al. (2005) Brain tumor tropism of transplanted human neural stem cells is induced by vascular endothelial growth factor. *Neoplasia* 7:623–629.
- Widera D, et al. (2004) MCP-1 induces migration of adult neural stem cells. *Eur J Cell Biol* 83:381–387.
- Palumbo R, et al. (2007) Cells migrating to sites of tissue damage in response to the danger signal HMGB1 require NF-kappaB activation. *J Cell Biol* 179:33–40.
- Stagg J, Lejeune L, Paquin A, Galipeau J (2004) Marrow stromal cells for interleukin-2 delivery in cancer immunotherapy. *Hum Gene Ther* 15:597–608.
- Kucerova L, Altanerova V, Matuskova M, Tyciakova S, Altaner C (2007) Adipose tissue-derived human mesenchymal stem cells mediated prodrug cancer gene therapy. *Cancer Res* 67:6304–6313.
- Sonabend AM, et al. (2008) Mesenchymal stem cells effectively deliver an oncolytic adenovirus to intracranial glioma. *Stem Cells* 26:831–841.
- Almasan A, Ashkenazi A (2003) Apo2L/TRAIL: apoptosis signaling, biology, and potential for cancer therapy. *Cytokine Growth Factor Rev* 14:337–348.
- Germano IM, Uzzaman M, Benveniste RJ, Zurova M, Keller G (2006) Apoptosis in human glioblastoma cells produced using embryonic stem cell-derived astrocytes expressing tumor necrosis factor-related apoptosis-inducing ligand. *J Neurosurg* 105:88–95.
- Panner A, James CD, Berger MS, Pieper RO (2005) mTOR controls FLIPLS translation and TRAIL sensitivity in glioblastoma multiforme cells. *Mol Cell Biol* 25:8809–8823.
- Griffith TS, Anderson RD, Davidson BL, Williams RD, Ratliff TL (2000) Adenoviral-mediated transfer of the TNF-related apoptosis-inducing ligand/Apo-2 ligand gene induces tumor cell apoptosis. *J Immunol* 165:2886–2894.
- Kagawa S, et al. (2001) Antitumor activity and bystander effects of the tumor necrosis factor-related apoptosis-inducing ligand (TRAIL) gene. *Cancer Res* 61:3330–3338.
- Shah K, et al. (2005) Glioma therapy and real-time imaging of neural precursor cell migration and tumor regression. *Ann Neurol* 57:34–41.
- Dirks PB (2005) Brain tumor stem cells. *Biol Blood Marrow Transplant* 11:12–13.
- Shah K, Tang Y, Breakefield X, Weissleder R (2003) Real-time imaging of TRAIL-induced apoptosis of glioma tumors in vivo. *Oncogene* 22:6865–6872.
- Kock N, Kasimieh R, Weissleder R, Shah K (2007) Tumor therapy mediated by lentiviral expression of shBcl-2 and S-TRAIL. *Neoplasia* 9:435–442.
- Wakimoto H, et al. (2009) Human glioblastoma-derived cancer stem cells: Establishment of invasive glioma models and treatment with oncolytic herpes simplex virus vectors. *Cancer Res*, in press.